4522 *Inorg. Chem.* **1994**, *33*, 4522−4530

Heterocyclic Systems Containing Tin(IV). 10.[1] Control of Three-Center Interactions X···Sn−Hal in Stannocanes by Halide Type[†]

Ute Kolb, Mike Beuter, and Martin Dräger*

Institut für Anorganische Chemie und Analytische Chemie der Johannes Gutenberg-Universität, D-55099 Mainz, Germany

Received February 15, 1994[®]

The stannocanes $Cl_2/Br_2/I_2{-}Sn(SCH_2CH_2)_2X$ (X = NMe, O, S) have been synthesized from $SnHal_4$ and $(HSCH_2CH_2)_2X$. Assigned vibrational (IR and Raman) and NMR data (^{13}C and ^{119}Sn) and, for X = O and S, crystal structure determinations are given. All nine compounds comprise molecules in which the tin atom approaches a trigonal-bipyramidal pentacoordination with 2×S and Hal_{eq} as equatorial ligands and with X and Hal_{ax} as axial ligands. The latter two bonds are described by means of a three-center, four-electron interaction X···Sn−Hal for which a qualitative MO description in terms of frontier orbitals is given. A "path" from a tetrahedron to a trigonal bipyramid is controlled by four electronic factors (donor strength of X, electronegativity of Hal_{ax}, lone pair interaction of Hal_{ax}, type of equatorial ligands) and one steric factor (geometrical flexibility of X). These influences are discussed with respect to the structural and spectroscopic data (Pauling-type bond orders BO(X···Sn) and BO(Sn−Hal), geometrical goodness of the trigonal bipyramids, force constants *f*(Sn−Hal), and ^{119}Sn-NMR chemical shifts) of the nine compounds and are compared with the data of five analogous series taken from the literature. Regarding the influence of Hal_{ax}, the factors "electronegativity" and "lone pair interaction" are counteractive and cancel each other, between bromine and iodine. The donor strength of X in the nine compounds decreases in the following orders: NMe > S ≥ O in the solid state and NMe > O > S in solution.

Introduction

For a long time we[2] and other groups[3,4] have dealt with eight-membered heterocycles $(R,R')M(SCH_2CH_2)_2X$. These rings consist of a Lewis acidic acceptor atom M (Ge, Sn, Pb, As, Sb, or Bi) and of a donor group X (NR″, O, S, or Se). A 1,5-transannular interaction between M and X leads to an increase of the coordination number of M.[5] Recently we showed that for a special series of five-coordinated triorganotin compounds coordinating Sn···O distances decrease in the order of trans substituents F > Cl = Br > I, with the shortest Sn···O distances of 2.39 Å in the case of iodine.[6] Contrary to this result, Dostal et al.[7] found that for a series of monoorganotin compounds coordinating Sn···O distances are in the order F < Cl < Br, with the shortest Sn···O of 2.40 Å in the case of fluorine. For clarification, we returned to our old compound series and synthesized the tin compounds $Hal_2Sn(SCH_2CH_2)_2X$ (**1a**−**3c**). Crystal structures and vibrational and NMR data will be used to ascertain the strength of the Lewis acidity of tin in these compounds.

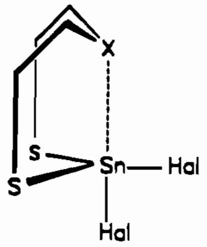

1, 2, 3

X	Hal = Cl	Hal = Br	Hal = I
NMe	**1a**	**1b**	**1c**
O	**2a**	**2b**	**2c**
S	**3a**	**3b**	**3c**

Results

Synthesis. The compounds **1a**−**3c** have been synthesized by means of standard procedures[5] from $SnHal_4$ and MeN/O/$S(CH_2CH_2SH)_2$. The synthesis of $MeN(CH_2CH_2SH)_2$[8,9] has been optimized. Apart from **3c**, which decomposes even upon cooling within a few days (changing from a golden yellow to a pale yellow color), the other eight compunds are stable at room temperature and in air; the iodine compounds are light sensitive. The compounds are slightly soluble in nonpolar solvents, except the iodine-substituted series, which is only sparingly soluble and decomposes in solution. Additionally, the solubility of the three compounds **1** (X = NMe) is distinctly

---

[†] Dedicated to Prof. Philipp Gütlich, on the occasion of his 60th birthday. Parts of the intended Ph.D. theses of U.K. and M.B. are included.

[®] Abstract published in *Advance ACS Abstracts*, August 1, 1994.

(1) Part 9: Dräger, M. Z. *Naturforsch.* **1985**, *40B*, 1511.

(2) Dräger, M.; Engler, R. *Z. Anorg. Allg. Chem.* **1974**, *405*, 183.

(3) (a) Tzschach, A.; Pönicke, K. *Z. Anorg. Allg. Chem.* **1974**, *404*, 121. Mügge, C.; Jurkschat, K.; Tzschach, A.; Zschunke, A. *J. Organomet. Chem.* **1979**, *164*, 135. Review: Tzschach, A.; Jurkschat, K. *Comments Inorg. Chem.* **1983**, *3*, 35. (b) Swisher, R. G.; Holmes, R. R. *Organometallics* **1984**, *3*, 365. Review on five-coordinated structures: Holmes, R. R. *Prog. Inorg. Chem.* **1984**, *32*, 119.

(4) For the extensive related work of further groups, cf. the references cited in recent articles: (a) Jastrzebski, J. T. B. H.; van der Schaaf, P. A.; Boersma, J.; van Koten, G. *Organometallics* **1992**, *11*, 1521. (b) Dakternieks, D.; Zhu, H.; Masi, D.; Mealli, C. *Inorg. Chem.* **1992**, *31*, 3601. (c) Wan, Y.; Verkade, J. G. *Inorg. Chem.* **1993**, *32*, 79.

(5) Dräger, M.; Guttmann, H.-J. *J. Organomet. Chem.* **1981**, *212*, 171.

(6) Kolb, U.; Dräger, M.; Jousseaume, B. *Organometallics* **1991**, *10*, 2737.

(7) Dostal, S.; Stoudt, S. J.; Fanwick, P.; Sereatan, W. F.; Kahr, B.; Jackson, J. E. *Organometallics* **1993**, *12*, 2284.

(8) Eisleb, O. *Ber. Dtsch. Chem. Ges.* **1941**, *74*, 1433.

(9) Harley-Mason, J. *J. Chem. Soc.* **1947**, *320*.

0020-1669/94/1333-4522$04.50/0

Table 1. Bond Lengths, Bond Angles, and Torsion Angles of the Coordination Polyhedra at the Central Tin Atom and for the Eight-membered Rings in $Hal_2Sn(SCH_2CH_2)_2X$, (X = O (**2**), S (**3**); Hal = Br (**b**), I (**c**)) and for Comparison in $Cl_2Sn(SCH_2CH_2)_2X$ (**2a, 3a**)

	X = O			X = S		
	2a (Hal = Cl)[a]	**2b** (Hal = Br)	**2c** (Hal = I)	**3a** (Hal = Cl)[a]	**3b** (Hal = Br)	**3c** (Hal = I)
(a) Coordination Polyhedra						
Bond Lengths (Å)[b]						
Sn—Hal(ax)	2.376(3)	2.536(2)	2.738(1)	2.392(3)	2.545(1)	2.786(1)
Sn—Hal(eq)	2.346(3)	2.477(2)	2.682(1)	2.348(3)	2.491(1)	2.700(1)
Sn···X	2.359(6)	2.41(1)	2.431(5)	2.760(3)	2.767(2)	2.779(2)
Sn—S(1)	2.369(3)	2.361(3)	2.382(2)	2.386(3)	2.399(2)	2.393(2)
Sn—S(2)	2.369(3)	2.361(3)	2.380(2)	2.388(3)	2.400(2)	2.402(2)
Bond Angles (deg)						
Hal(ax)—Sn···X	170.9(2)	165.8(2)	166.4(1)	165.6(1)	174.5(1)	177.6(1)
Hal(ax)—Sn—Hal(eq)	99.8(2)	103.8(1)	106.1(1)	95.5(1)	96.2(1)	94.9(1)
Hal(ax)—Sn—S(1)	97.0(2)	95.7(1)	97.1(1)	91.6(1)	90.8(1)	96.5(1)
Hal(ax)—Sn—S(2)	97.0(2)	95.7(1)	97.1(1)	100.0(1)	100.2(1)	95.7(1)
X···Sn—Hal(eq)	89.3(2)	90.4(2)	87.6(1)	85.8(1)	86.1(1)	86.9(1)
X···Sn—S(1)	80.0(2)	79.5(1)	77.8(1)	84.0(1)	83.7(1)	84.0(1)
X···Sn—S(2)	80.0(2)	79.5(1)	77.9(1)	83.4(1)	83.4(1)	82.1(1)
Hal(eq)—Sn—S(1)	108.3(2)	108.4(1)	110.2(1)	117.6(1)	118.7(1)	115.7(1)
Hal(eq)—Sn—S(2)	108.3(2)	108.4(1)	109.2(1)	113.4(1)	113.0(1)	122.0(1)
S(1)—Sn—S(2)	137.7(2)	137.4(1)	132.2(1)	126.2(1)	125.4(1)	119.5(1)
(b) Eight-Membered Rings						
Bond Lengths (Å)						
S(1)—C(1)	1.82(1)	1.82(1)	1.83(1)	1.83(1)	1.80(1)	1.82(1)
C(1)—C(2)	1.48(1)	1.51(2)	1.51(1)	1.51(1)	1.51(1)	1.50(2)
C(2)—X	1.45(1)	1.44(1)	1.44(1)	1.81(1)	1.82(1)	1.81(1)
X—C(3)	1.45(1)	1.44(1)	1.42(1)	1.82(1)	1.80(1)	1.80(1)
C(3)—C(4)	1.48(1)	1.51(2)	1.51(1)	1.51(1)	1.54(1)	1.55(1)
C(4)—S(2)	1.82(1)	1.82(1)	1.85(1)	1.81(1)	1.82(1)	1.83(1)
Bond Angles (deg)						
Sn—S(1)—C(1)	97.4(3)	97.1(3)	98.1(3)	99.0(2)	103.7(3)	101.1(4)
S(1)—C(1)—C(2)	112.4(6)	113.3(8)	112.4(6)	114.0(3)	115.1(6)	115.0(7)
C(1)—C(2)—X	107.5(6)	106.0(8)	107.8(6)	114.6(3)	110.8(6)	112.4(6)
C(2)—X—C(3)	111.0(6)	113.9(7)	115.1(6)	104.2(2)	104.0(4)	104.0(5)
X—C(3)—C(4)	107.5(6)	106.0(8)	107.8(6)	109.0(3)	114.5(5)	113.6(6)
C(3)—C(4)—S(2)	112.4(6)	113.3(8)	111.2(5)	115.1(3)	113.9(5)	111.4(6)
C(4)—S(2)—Sn	97.4(3)	97.1(3)	97.6(3)	102.3(2)	99.1(3)	97.4(3)
Torsion Angles (deg)						
S(2)—Sn—S(1)—C(1)	−826	−83.8(5)	−85.9(3)	−907	88.9(3)	98.2(4)
Sn—S(1)—C(1)—C(2)	499	53.1(8)	53.7(6)	504	−46.9(6)	−54.9(6)
S(1)—C(1)—C(2)—X	−599	−60.3(1)	−56.5(7)	−697	67.3(7)	66.0(8)
C(1)—C(2)—X—C(3)	1697	170.5(1)	171.5(7)	1447	−144.7(6)	−136.0(8)
C(2)—X—C(3)—C(4)	−1697	−170.5(1)	−172.7(7)	−745	73.4(7)	76.0(7)
X—C(3)—C(4)—S(2)	599	60.3(1)	57.7(7)	−598	60.5(7)	62.8(6)
C(3)—C(4)—S(2)—Sn	−499	−53.1(8)	−54.3(5)	609	−60.4(5)	−66.6(6)
C(4)—S(2)—Sn—S(1)	826	83.8(5)	86.3(3)	466	−46.8(3)	−42.7(3)
Ring Conformations[c]						
	CC	CC	CC	CB	CB	CB

[a] See ref 10. [b] Shortest intermolecular distances: **2a**, *d*(Sn···Cl) = 4.260 Å; **2b**, *d*(Sn···Br) = 5.375 Å; **2c**, *d*(Sn···I) = 4.528 Å; **3a**, *d*(Sn···S) = 4.231 Å; **3b**, *d*(Sn···S) = 4.336 Å; **3c**, *d*(Sn···S) = 5.124 Å. [c] C = chair; B = boat.

less than that for the other cases (X = O and S). Along with the low solubility, the melting points of the three compounds **1** are distinctly higher than those of the series **2** and **3**.

Molecular Structures. The structure determinations of $Hal_2Sn(SCH_2CH_2)_2O$ (Br, **2b**; I, **2c**) and $Hal_2Sn(SCH_2CH_2)_2S$ (Br, **3b**; I, **3c**) reveal pentacoordinate tin. The geometrical properties of these compounds and a comparison with $Cl_2Sn(SCH_2CH_2)_2O$ (**2a**) and $Cl_2Sn(SCH_2CH_2)_2S$ (**3a**) are given in Table 1. In both series (**2a/2b/2c**) and (**3a/3b/3c**) the individual molecules differ only slightly. Figure 1 gives exemplarily plots of the two bromine-substituted cases. In all six compounds the coordination around tin approaches a trigonal bipyramid. Details will be discussed below along with the spectroscopic data. The conformations of the eight-membered rings are three times chair—chair (X = O, Figure 1 left; perfect mirror plane for **2b** by space group) and three times boat—chair (X = S, Figure 1

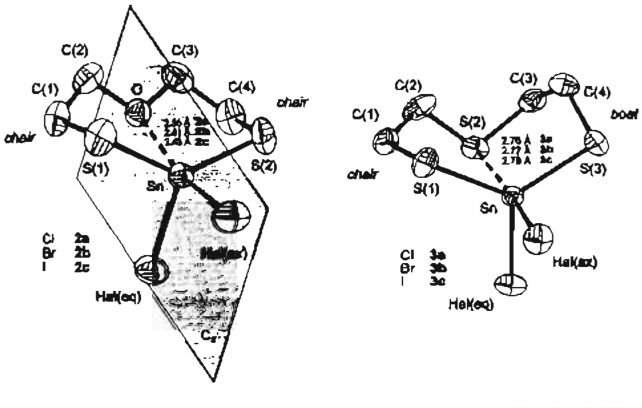

Figure 1. Intramolecular coordination in the compounds $Hal_2Sn(SCH_2CH_2)_2X$ (Hal = Cl (**2a**, **3a**), Br (**2b**, **3b**), I (**2c**, **3c**)). Labels of atoms are as given in Tables 1 and 2. ORTEP drawings are exemplary of **2b** (left) and **3b** (right); thermal ellipsoids are at the 50% probability level. Hydrogen atoms are omitted for better clarity. The C_s mirror plane in **2b** is outlined.

---

(10) Dräger, M.; Engler, R. *Z. Anorg. Allg. Chem.* **1975**, *413*, 229; *Chem. Ber.* **1975**, *108*, 17.

Table 2. Spectroscopic Data for the Stannocanes $Hal_2Sn(SCH_2CH_2)_3X$ (Hal = Cl (**a**), Br (**b**), I (**c**); X = NMe (**1**), O (**2**), S (**3**))

		X = NMe			X = O			X = S		
assign[a]		**1a** (Hal = Cl)	**1b** (Hal = Br)	**1c** (Hal = I)	**2a** (Hal = Cl)	**2b** (Hal = Br)	**2c** (Hal = I)	**3a** (Hal = Cl)	**3b** (Hal = Br)	**3c** (Hal = I)[b]
				(a) Stretching Vibrations ν (cm^{-1}) for the Coordination Polyhedra at Tin						
$\nu(SnS_2)_{as}$	IR	388 s (97)[c]	386 m (100)	378 vs (100)	395 s (74)[c]	390 vs (100)	378 vs (100)	377 s (85)[c]	368 vs (98)	
	Raman	389 m (22)[c]	386 m (23)	378 m (15)	401 m (10)[c]	393 m (18)	381 m (11)	382 m (13)[c]	373 m (23)	
$\nu(SnS_2)_s$	IR	343 s (90)	340 s (70)	336 s (37)	367 s (78)	359 vs (95)	352 s (82)	328 s (80)	335 s (81)	
	Raman	345 s (42)	337 s (46)	328 s, br (23)	368 vs (100)	365 vs (100)	358 s (40)	325 vs (100)	335 vs (100)	
$\nu(Sn\text{-}Hal_{eq})$	IR	324 s (74)[c]	230 s (56)	*d*	351 s (76)[c]	*d*	210 s, br (95)	352 vs (100)[c]	242 s (78)	
	Raman	326 vs (100)[c]	227 vs (76)	183 s (38)	346 s (66)[c]	243 s (54)	203 m (16)	351 s (26)[c]	237 s (47)	
$\nu(Sn\text{-}Hal_{ax})$	IR	293 s (100)	*d*	*d*	326 vs (100)	*d*	163 vs (98)	311 vs br (92)	208 s (100)	
	Raman	295 s (22)	163 vs (74)	140 vs (90)	321 s, br (35)	208 s (61)	173 vs (100)	312 sh (11)	209 vs (77)	
$\nu(S\cdot\cdot Sn)$	IR	*e*	*e*	*e*	335 sh (98)	335 w (69) 302 w (65)	325 m (37) 305 s (68)	135 m (67)	*d*	
	Raman	*e*	*e*	*e*	306 m (15)	308 m (29)	309 m (7)	132 m (17)	128 m (27)	
				(b) ^{13}C-NMR Data (δ (ppm), $J(^{13}C-^{119}Sn)$ (Hz))[f,g]						
$\delta(^{\beta}C)$, $S-CH_2$		25.2	26.0	27.5	29.4	30.4	31.6	28.9	29.2	30.2
^2J		26.7	27.7	*h*	33.8	30.9	30.3	35.3	35.3	35.9
$\delta(^{\gamma}C)$, CH_2-X		56.5	55.8	54.9	70.5	70.5	70.0	39.3	39.3	40.3
^3J		91.3	88.8	*h*	36.8	33.8	26.2	35.3	29.4	23.8
$\delta(N-Me)$		43.5	43.9	44.7						
^5J		8.8	10.4	*h*						
				(c) ^{119}Sn-NMR Data (δ (ppm))[f]						
$\delta(^{119}Sn)$	−139.0[i]	*h*	*h*	*h*	−132.0	−40.9	−589.9	−122.2	14.1	−567.6[i]

[a] Intensities of vibrations in parentheses (relative peak height intensities). [b] **3c** decomposes; no reliable vibrational data obtainable. [c] A coupling between $\nu(SnS_2)_{as}$ and $\nu(SnHal_{eq})$ may be assumed. [d] IR < 200 cm^{-1} not measured. [e] Hidden by $\nu(SnS_2)$. [f] Solvent: $CDCl_3$ (**2**, **3**), CD_2Cl_2 (**1**). [g] Starting compounds $(HSCH_2CH_2)_2X$: X = NMe/O/S, $\delta(^{\beta}C)$ = 22.6/23.9/24.4, $\delta(^{\gamma}C)$ = 60.1/71.8/35.3, $\delta(N-Me)$ = 41.4 (ppm). [h] Low solubility of the compound and decomposition in solution. [i] Exchange-broadened signal.

Scheme 1

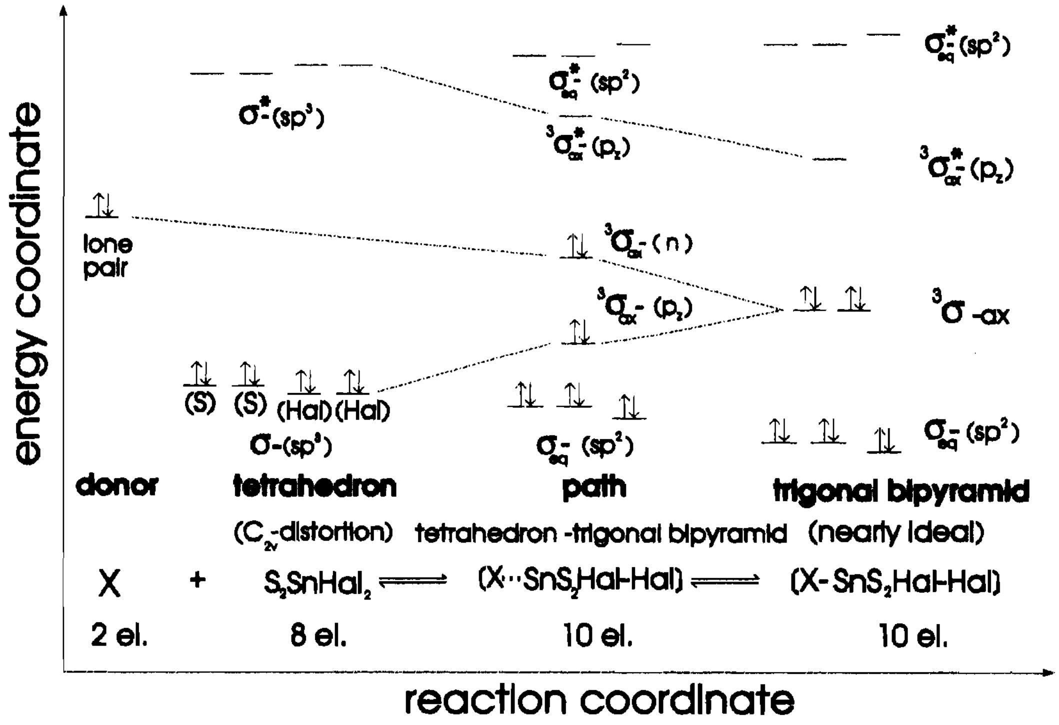

right). Compounds **2** and **3** exhibit no short intermolecular interactions. In contrast, such an expansion of the coordination sphere should be assumed for compounds **1** on account of theirlow solubilities and high melting points.

Vibrational Data. A full set of assigned IR and Raman transitions down from 600 cm^{-1} for eight compounds of the series **1**–**3** (**3c** decomposes; no reliable data obtainable) has been determined. Table 2 shows the five stretching frequencies of the coordination polyhedra for tin; for the other data see the supplementary material. The stretching vibrations of a trigonal bipyramid should show no coupling between axial and equatorial ligands. For **1a**, **2a**, and **3a** a coupling between $\nu(Sn-Cl_{eq})$ and $\nu(Sn-S_2)_{as}$ may by assumed.

NMR Data. The ^{13}C and ^{119}Sn NMR data are summarized in Table 2. The spin–spin coupling $^3J(^{13}C-^{119}Sn)$ (mode of coupling $Sn-S-CH_2-CH_2$) can alternatively be viewed as $^2J(^{13}C-^{119}Sn)$ (mode of coupling $Sn\cdot\cdot X-CH_2$). Correspondingly, ^5J may be viewed as ^3J (way of coupling $Sn\cdot\cdot N-CH_3$).

Table 3. Structural Features of the Three-Center Interaction $X{\cdot\cdot}Sn{-}Hal_{ax}$ along Series **2** and **3** and along Five Analogous Series (**4**,[6] **5**,[13] **6**,[14] **7**,[7] **8**−**10**[15]) from the Literature (Distances in Å, $\Delta\Sigma(\vartheta)$ in deg)

compd	X	$d(X{\cdot\cdot}Sn)$	$\Delta d(X{\cdot\cdot}Sn)$ bond widening[a]	Hal	$d(Sn{-}Hal_{ax})$	$\Delta d(Sn{-}Hal)$ bond widening[a]	Pauling-type bond order[b]		geometrical goodness of the trigonal bipyramid[c]	
							$BO(X{\cdot\cdot}Sn)$	$BO(Sn{-}Hal)$	$\Delta\Sigma(\vartheta)$	$\Delta Sn(plane)$
3a	S	2.760(3)	0.36	Cl	2.392(3)	0.03	0.31	0.91	70	0.21
3b		2.767(2)	0.37	Br	2.545(1)	0.05	0.30	0.85	70	0.21
3c		2.779(2)	0.38	I	2.786(1)	0.08	0.29	0.77	70	0.21
2a	O	2.359(6)	0.36	Cl	2.376(3)	0.02	0.31	0.94	61	0.29
2b		2.41(1)	0.41	Br	2.536(2)	0.04	0.27	0.88	59	0.29
2c		2.431(5)	0.43	I	2.738(1)	0.03	0.25	0.91	51	0.36
4a	CO	2.470(3)	0.47	Cl	2.432(1)	0.07	0.22	0.80	57	0.33
4b		2.470(6)	0.47	Br	2.588(1)	0.09	0.22	0.75	55	0.34
4c		2.391(5)	0.39	I	2.830(7)	0.12	0.28	0.68	56	0.33
4d		2.52(1)	0.52	F	1.974(8)	0.02	0.19	0.94	66	0.25
5a (hex)	N	2.37(2)	0.28	Cl	2.519(7)	0.16	0.41	0.59	49	0.39
5a (mon)		2.384(4)	0.29		2.554(1)	0.19	0.39	0.54	50	0.38
5b		2.284(2)	0.19	Br	2.693(2)	0.19	0.54	0.54	55	0.33
5c		2.375(6)	0.29	I	2.896(1)	0.19	0.39	0.54	53	0.35
5d (Dim 1)		2.427(6)	0.34	F	2.122(5)	0.17	0.33	0.58	49	0.41
5d (Dim 2)		2.393(5)	0.30		2.115(6)	0.17	0.38	0.58	50	0.38
6a	N_{ar}	2.668(3)	0.58	Cl	2.452(2)	0.09	0.31[d]	0.75	70	0.16
6b		2.653(5)	0.56	Br	2.619(1)	0.12	0.32[d]	0.68	70	0.27
6c		2.655(7)	0.57	I	2.830(1)	0.12	0.32[d]	0.68	68	0.23
7a1	O	2.555(7)	0.56	Cl	2.400(3)	0.04	0.16	0.88	*e*	*e*
7a2		2.640(7)	0.64		2.374(3)	0.01	0.13	0.97	*e*	*e*
7a3		2.593(7)	0.59		2.390(3)	0.03	0.15	0.91	*e*	*e*
7a1′		2.603(7)	0.60		2.377(3)	0.02	0.14	0.94	*e*	*e*
7a2′		2.576(7)	0.58		2.393(2)	0.03	0.15	0.91	*e*	*e*
7a3′		2.611(7)	0.61		2.386(3)	0.03	0.14	0.91	*e*	*e*
7b1		2.592(3)	0.59	Br	2.511(1)	0.01	0.15	0.97	*e*	*e*
7b2		2.606(4)	0.61		2.532(1)	0.02	0.14	0.94	*e*	*e*
7b3		2.760(4)	0.76		2.543(1)	0.04	0.09	0.88	*e*	*e*
7d1		2.454(7)	0.45	F	1.956(6)	0.01	0.23	0.97	*e*	*e*
7d2		2.455(8)	0.46		1.948(7)	0.00	0.23	1.00	*e*	*e*
7d3		2.399(7)	0.40		1.975(6)	0.03	0.28	0.91	*e*	*e*
8d	PO	2.454(3)	0.45	F	2.035(2)	0.09	0.55	0.75	73	0.19
9b	PS	2.872(2)	0.47	Br	2.650(1)	0.15	0.53	0.61	78	0.14
10a	PSe	3.022(1)	0.47	Cl	2.500(3)	0.14	0.53	0.68	77	0.14

[a] According to standard single-bond distances $d(Se{-}Sn) = 2.55$, $d(S{-}Sn) = 2.40$, $d(O{-}Sn) = 2.00$, $d(N{-}Sn) = 2.09$, $d(Sn{-}F) = 1.95$, $d(Sn{-}Cl) = 2.36$, $d(Sn{-}Br) = 2.50$, and $d(Sn{-}I) = 2.71$ Å.[18] [b] Mode of calculation $BO = 10^{-(\Delta d-1.41)}$,[16] equivalent to the creation of a bond according to intramolecularly nonbonding distances $d(S{-}Sn) + 1.00$ Å $= 3.40$ Å, $d(O{-}Sn) + 1.00$ Å $= 3.00$ Å, and $d(N{-}Sn) + 1.00$ Å $= 3.09$ Å.[17] [c] "Steric path" from a tetrahedron [$\Delta\Sigma(\theta) = 0°$, $\Delta Sn(plane) = 0.71$ Å] to a trigonal bipyramid [$\Delta\Sigma(\theta) = 90°$, $\Delta Sn(plane) = 0.00$ Å].[6,21] [d] Mode of calculation $BO = 10^{-(\Delta d-1.41/1.60)}$,[16] equivalent to the creation of a bond according to an intermolecularly nonbonding distance (van der Waals distance) of $d(N{-}Sn) + 1.60$ Å $= 3.69$ Å.[17] [e] Monocapped octahedral heptacoordination.

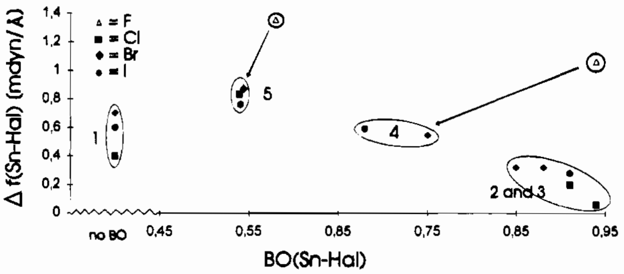

Figure 2. Plot of the weakening of force constant $\Delta f(Sn{-}Hal)$ versus Pauling-type bond order $BO(Sn{-}Hal)$. (Coinciding symbols for **5** were slightly spread to obtain transparency; see Tables 3 and 4).

Discussion

Hypervalent Bonds. As first outlined in detail by Musher,[11] hypervalent bonds of a main group element M can be described by means of three-center interactions $^3\sigma$: L(trans)−M−L(trans).

Regarding the case $X{\cdot\cdot}Sn{-}Hal$, Scheme 1 gives a qualitative MO description in terms of frontier orbitals (cf. related qualitative descriptions of stannate anions[12a] and of ψ-trigonal bipyramidal coordinated bismuth(III) anions and cations[12b,c]). The donor X (lone pair orbital) interacts with the tetrahedral moiety S_2SnHal_2 (four sp^3-hybridized σ orbitals and four σ^* orbitals), forming a "path" to a trigonal bipyramid. The path consists of three equatorial sp^2-hybridized σ orbitals, three axial three-center orbitals $^3\sigma$ (one strongly bonding $^3\sigma(p_z)$, one weakly bonding $^3\sigma(n)$ HOMO, one antibonding $^3\sigma^*(p_z)$ LUMO), and three equatorial σ^* orbitals. In achieving the "path", the two bonding $^3\sigma$ orbitals come closer together and the $^3\sigma^*$ LUMO becomes progressively lower; concomitantly, a strengthening

---

(11) Musher, J. I. *Angew. Chem.* **1969**, *81*, 68; *Angew. Chem., Int. Ed. Engl.* **1969**, *8*, 54. Cf. also: Kutzelnigg, W. *Angew. Chem.* **1984**, *96*, 262; *Angew. Chem., Int. Ed. Engl.* **1984**, *23*, 272.

(12) (a) Suzuki, M.; Son, I.-H.; Noyori, R.; Masuda, H. *Organometallics* **1990**, *9*, 3043. (b) Clegg, W.; Compton, N. A.; Errington, R. J.; Fisher, G. A.; Hockless, D. C. R.; Norman, N. C.; Orpen, A. G.; Stratford, S. E. *J. Chem. Soc., Dalton Trans.* **1992**, 3515. Carmelt, C. J.; Norman, N. C.; Orpen, A. G.; Stratford, S. E. *J. Organomet. Chem.* **1993**, *460*, C22. (c) Cf. also for the bonding of PR_3 to transition metals: Orpen, A. G.; Connelly, N. G. *J. Chem. Soc., Chem. Commun.* **1985**, 1310. (d) For recent work on the related case of boron halides, cf.: Brinck, T.; Murray, J. S.; Politzer, P. *Inorg. Chem.* **1993**, *32*, 2622.

of the three equatorial orbitals occurs. According to the orbitals involved, four electronic effects control the "path". The donor X shifts charge into $^3\sigma(n)$ and lowers it ("donor strength": path to the right). The axial ligand $\mathrm{Hal_{ax}}$ removes charge from $^3\sigma(p_z)$ and raises it ("electronegativity": path to the right; in the concerned case along the series I < Br < Cl < F). A "movable" charge at the axial ligand $\mathrm{Hal_{ax}}$ interacts with the antibonding LUMO $^3\sigma^*(p_z)$ ("lone pair interaction": path to the left; in the concerned case along the series I < Br < Cl < F). An enhanced electronegativity of the equatorial ligands (2 × S, $\mathrm{Hal_{eq}}$) lowers their orbitals ("equatorial ligands": path to the right). In addition to the electronic control ("electronic path"), a steric control (geometrical flexibility of the donor X: "steric path") should be regarded. In a recent reference about the related case of boron halides the so-called "charge capacity" of an acceptor molecule is used, which can be compared with a combination of the four electronic effects in one factor.[12d]

Influence of the Halide. Table 3 summarizes the structural aspects of the "path" of Scheme 1 for the compound series **2** and **3** and compares them with those of five analogous series taken from the literature: **4**[6], **5**,[13] **6**[14] (intermolecular coordination), **7**[7] (3× a three-center interaction with monocapped octahedral heptacoordinated tin), and **8**–**10**.[15] The "electronic path" is described in terms of exponential Pauling-type bond orders:[16] BO = 1.00 for a standard single-bond distance *d*(single); BO = 0.04 for the lower limits[17] of intramolecularly nonbonding distances (*d*(single) + 1.00 Å) or of intermolecularly (van der Waals) nonbonding distances (*d*(single) + 1.60 Å). The value "1.00 (or 1.60 for **6**) − Δd(X···Sn)" accounts for a lowering of $^3\sigma(n)$ resulting in an increase of BO(X···Sn). The bond widening Δd(Sn—Hal) accounts for a raising of $^3\sigma(p_z)$ resulting in a decresae of BO(Sn—Hal). The standard single-bond distances *d*(single X—Sn) were calculated from the radii of O'Keeffe and Brese;[18] a correction for electronegativity has been omitted. These values (footnote *a* in Table 3) are in good agreement with experimental data.[19] The radius of iodine in ref 18 seems to be too long; the Sn—I distance in $\mathrm{Mes_3SnI}$[20] has been chosen as a standard. The "steric path" is described in terms of $\Delta\Sigma(\Theta)$,[6,21] the difference between the three equatorial angles and the three axial angles involving $\mathrm{Hal_{ax}}$, and in terms of ΔSn(plane),[6] the deviation of the tin atom from the plane through the three equatorial ligands (correction to a standard distance of 2.10 Å for all ligands).

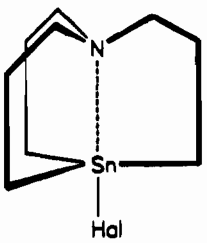

5

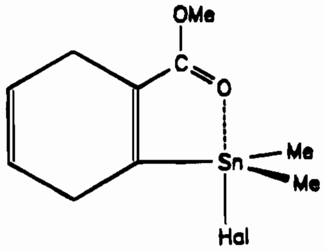

4

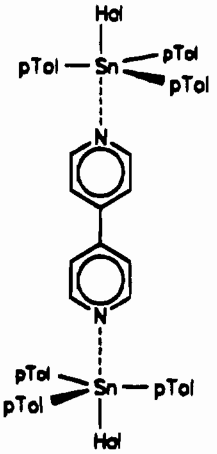

6

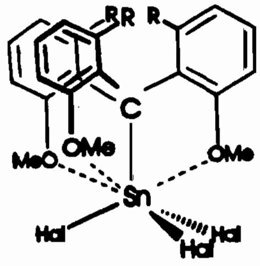

R = OMe

7

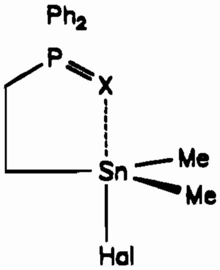

8, 9, 10

X	Hal = Cl	Hal = Br	Hal = I	Hal = F
CO	**4a**	**4b**	**4c**	**4d**
N	**5a**	**5b**	**5c**	**5d**
$\mathrm{N_{ar}}$	**6a**	**6b**	**6c**	
O	**7a**	**7b**	**7c**	**7d**
PO				**8d**
PS		**9b**		
PSe	**10a**			

BO(Sn—Hal) generally follows BO(X···Sn), but the resolution of BO(Sn—Hal) is better. No direct connection between the "electronic path" and the "steric path" exists. The strained molecules **5** have the highest BO(X···Sn) and the lowest BO(Sn—Hal), and yet their structures deviate mainly from a geometrical trigonal bipyramid. For the steric behavior of such compounds like **8**–**10**, see ref 22.

Table 4 describes the path of Scheme 1 in terms of vibrational and ^{119}Sn-NMR data. From the stretching vibrations ν(Sn—Hal) simplified force constants *f*(Sn—Hal) were calculated (approximation of a diatomic oscillator[23] with masses of tin and halide: "mass-corrected stretching vibration"), and the latter are compared with standard single-bond force constants for $\mathrm{Me_3SnHal}$ (values in footnote *b* of Table 4 calculated in the same

---

(13) Kolb, U.; Dräger, M.; Jurkschat, K. *Organometallics*, in preparation.

(14) Bajue, S. A.; Bramwell, F. B.; Charles, M. A.; Cervantes-Lee, F.; Pannell, K. *Inorg. Chim. Acta* **1992**, *197*, 83.

(15) Preut, H.; Godry, B.; Mitchell, T. N. *Acta Crystallogr.* **1992**, *C48*, 1491, 1834, 1894.

(16) Pauling, L. *The Nature of the Chemical Bond*, 3rd ed.; Cornell University Press: Ithaca, NY, 1960; p 239. Cf. also: Dunitz, J. D. *X-Ray Analysis and the Structure of Organic Molecules*; Cornell University Press: Ithacha, NY, 1979; Chapter 7.

(17) Dräger, M. *Z. Anorg. Allg. Chem.* **1976**, *423*, 53.

(18) O'Keeffe, M.; Brese, N. E. *J. Am. Chem. Soc.* **1991**, *113*, 3226.

(19) (a) Al-Juaid, S. S.; Dhaher, S. M.; Eaborn, C.; Hitchcock, P. B.; Smith, J. D. *J. Organomet. Chem.* **1987**, *325*, 117. (b) Reuter, H.; Puff, H. *J. Organomet. Chem.* **1989**, *379*, 223. (c) Skinner, H. A.; Sutton, L. E. *Trans. Faraday Soc.* **1944**, *40*, 164 (gas phase distances in methyltin halides by electron diffraction). For a compilation of *d*(Sn—Hal) and evaluation as single-bond standards, see ref 6.

(20) Schneider-Koglin, C.; Dräger, M. Unpublished crystal structure determination of $\mathrm{Mes_3SnI}$, giving two crystallographically independent Sn—I distances of 2.707(3) and 2.715(3) Å.

(21) Dräger, M. *J. Organomet. Chem.* **1983**, *251*, 209.

(22) Kolb, U.; Dräger, M.; Fischer, E.; Jurkschat, K. *J. Organomet. Chem.* **1992**, *423*, 339.

(23) Colthup, N. B.; Daly, L. H.; Wiberley, S. E. *Introduction to Infrared and Raman Spectroscopy*, 2nd ed.; Academic Press: New York, San Francisco, London, 1975; p 180.

(24) Licht, K.; Geissler, H.; Koehler, P.; Hottmann, K.; Schnorr, H.; Kriegsmann, H. *Z. Anorg. Allg. Chem.* **1971**, *385*, 271 (gas phase value).

Table 4. Spectroscopic Features of the Three-Center Interaction X••Sn—Hal_{ax} along Series **1**–**3** and along Four Analogous Series (**4**,[6] **5**,[13] **6**,[14] **7**[7]) from the Literature (Average of IR and Raman Transitions, If Both Are Available)

compd		Hal	ν(Sn—Hal_{ax}), cm^{-1}	*f*(Sn—Hal_{ax})[a] mdyn/Å	Δ*f*(Sn—Hal),[b] weakening of force const	ν(X••Sn), cm^{-1}	δ(^{119}Sn)	trend
3a	S	Cl	311	1.56	0.20	134	−122.2	low field shift
3b		Br	208	1.22	0.32	128	14.1	
3c		I	*d*			*d*	−567.6	high field
2a	O	Cl	324	1.70	0.06	335/306[e]	−132.0	low field shift
2b		Br	208	1.22	0.32	335/304[e]	−40.9	
2c		I	168	1.01	0.28	325/305[e]	−589.9	high field
4d	CO	F	486	2.28	1.06		−41.9	high field
4a		Cl					−31.5	high field shift
4b		Br	188	0.99	0.55		−44.6	
4c		I	139	0.70	0.59		−79.6	
1a	NMe	Cl	294	1.38	0.38	*f*	−139.0	
1b		Br	163	0.75	0.79	*f*	*d*	
1c		I	140	0.71	0.58	*f*	*d*	
5d	N	F	454	1.99	1.35	368/373[g]	41.7	high field shift
5a		Cl	240[h]	0.93[h]	0.83[h]	374[h]	19.5	
5b		Br	156	0.69	0.85	374	1.2	
5c		I	121	0.53	0.76	374	−43.0	
7a[c]	O	Cl					−344	high field shift
7b[c]		Br					−387	
7c[c]		I					−393	

[a] Calculated in the approximation of a diatomic oscillator with masses of tin and the corresponding halide: $f = (\nu/1303)^2(M_{\text{Hal}}M_{\text{Sn}}/(M_{\text{Hal}} + M_{\text{Sn}}))$.[23] [b] According to standard single-bond force constant Me_3SnF $f = 3.34$ mdyn/Å ($\nu = 588\ \text{cm}^{-1}$),[24] Me_3Sn—Cl/Br/I $f = 1.76/1.54/1.29$ mdyn/Å ($\nu = 331/234/189\ \text{cm}^{-1}$);[25] calculation of the force constant as in footnote *a*. [c] No vibrational and for **7d** also no NMR data available. [d] Compound decomposes; no reliable data obtainable. [e] Two frequencies observed for the C_s-symmetric molecules. [f] Hidden by $\nu(\text{SnS})_2$. [g] Dimeric unit. [h] Monoclinic modification.

Table 5. Sequences of Shifting the "Path" of Scheme 1 to the Right by Varying the Axial Halides Cl, Br, and I According to Different Data: "=", No Shift; ">", Slight Shift; "≫", Distinct Shift

compd series	data	sequences
1 (X = NMe)	Δ*f*(Sn—Hal)	Br ≫ I ≫ Cl
2 (X = O)	BO(X••Sn)	Cl > Br > I
	BO(Sn—Hal)	Br > I > Cl
	Δ*f*(Sn—Hal)	Br > I ≫ Cl
3 (X = S)	BO(X••Sn)	Cl > Br > I
	BO(Sn—Hal)	I ≫ Br ≫ Cl
	Δ*f*(Sn—Hal)	Br > Cl
4 (X = CO)	BO(X••Sn)	I ≫ Br = Cl
	BO(Sn—Hal)	I ≫ Br > Cl
	Δ*f*(Sn—Hal)	I > Br
5 (X = N)	BO(X••Sn)	Br ≫ I = Cl[a] and > Cl[b]
	BO(Sn—Hal)	Br = I = Cl[a] and ≫ Cl[b]
	Δ*f*(Sn—Hal)	Br > Cl[a] > I
6 (X = N_{ar})	BO(X••Sn)	I = Br > Cl
	BO(Sn—Hal)	I = Br > Cl
7 (X = O)	BO(X••Sn)	1× Cl > 2× Cl = 1× Br > 2× Cl = 1× Br > 1× Cl > 1× Br[c]
	BO(Sn—Hal)	1× Cl = 1× Br > 3× Cl = 1× Br > 1× Cl > 1× Cl > 1× Br[c]

[a] Monoclinic modification of **5a**.[13] [b] Hexagonal modification of **5a**.[13] [c] Six values for **7a** (two independent molecules with three three-center interactions each) and three values for **7b**.[7]

simplified manner). The resulting Δ*f*(Sn—Hal) accounts for a raising of $^3\sigma(p_z)$ and is plotted in Figure 2 versus BO(Sn—Hal) (data for series **1** at the left border). Generally, a decrease in BO(Sn—Hal) corresponds to an increase in Δ*f*(Sn—Hal).

From a consideration of Figure 2, it is evident that all compounds with Hal = F demand special discussion. Such a discussion is reported in a recent article[13] and will not be repeated here. For the other compounds with Hal = Cl, Br, and I, sequences of shifting the "path" of Scheme 1 to the right according to the different entries of Tables 3 and 4 are given in Table 5. Considering all included compound series together, bromine is the most active halide, closely followed by iodine. The two effects, "electronegativity" and "lone pair interaction", are counteractive and cancel each other, between the two heavier halides. Each of the seven series demands detailed discussion. The three series of this study show clearly the sequence Br > I > Cl if the data from the Sn—Hal bond are considered. If X••Sn is considered, this sequence is reversed, but the differences are small (especially in the case of **3**) and can be attributed to steric influences. Series **4** and **6** are uniform with I > Br > Cl and I = Br > Cl, respectively. Series **7** behaves statistically. The most difficult case is series **5**; a detailed discussion was presented recently.[13]

Table 6. Distances (Å) and Vibrational Data (cm^{-1}) for the Equatorial Ligands along the Series **1**–**3**

compd	X	Hal	*d*(Sn—Hal_{eq})	*d*(Sn—S)[a]	ν(Sn—Hal_{eq})	ν(Sn—S)[b]
1a[c]	NMe	Cl			325	366
1b[c]		Br			228	362
1c[c]		I			172	355
2a	O	Cl	2.346(3)	2.369(3)	348	383
2b		Br	2.477(2)	2.361(3)	243	377
2c		I	2.682(1)	2.381(2)	206	367
3a	S	Cl	2.348(3)	2.386(3)	351	353
3b		Br	2.491(1)	2.400(2)	239	353
3c		I	2.700(1)	2.397(2)	*c*	*d*

[a] Average, as equal within esd's. [b] Average of $\nu(\text{SnS}_2)_{as}$ and $\nu(\text{SnS}_2)_s$ ("Mittelfrequenz").[31] [c] No distances available. [d] Decomposition of **3c**; no reliable data obtainable.

Vibrations ν(X••Sn). The stretching vibrations ν(X••Sn) between the donor X and tin (Table 4) appear in definite ranges of the spectra, at about 130 cm^{-1} for S••Sn, at about 320 cm^{-1} for O••Sn, and at about 375 cm^{-1} for N••Sn. These ranges are reasonable. A further discussion is omitted in this context due to the limited amount of data (cf. ref 26).

---

(25) Clark, R. J. H.; Davies, A. G.; Puddephatt, R. J. *J. Chem. Soc. A* **1968**, 1828 (values in cyclohexane solution).

(26) Hoffmann, H. M.; Dräger, M.; Schmidt, B. M.; Kleiner, N. *Spectrochim. Acta* **1986**, *42A*, 1255. Hoffmann, H. M.; Dräger, M. *J. Organomet. Chem.* **1987**, *320*, 273. Schenzel, K.; Kolbe, A.; Reich, P. *Monatsh. Chem.* **1990**, *121*, 615.

Table 7. Sequences of Shifting the "Path" of Scheme 1 to the Right by Varying the Donor Groups NMe, O, and S According to Different Data: "=", No Shift; ">", Slight Shift; "≫", Distinct Shift

compd series	data from axial ligands		NMR data in soln		data from equatorial ligands	
1a, **2a**, **3a** (Hal = Cl)	BO(X··Sn)	S = O	$\delta(^{119}Sn)$	NMe > O > S	$d(Sn-Hal)^b$	0 ≥ S
	BO(Sn—Hal)	S > O	$^3J(^{13}C-^{119}Sn)^a$	NMe ≫ O > S	$d(Sn-S)^b$	O > S
	Δf(Sn—Hal)	NMe ≫ S ≫ O			ν(Sn—Hal)	S ≥ O ≫ NMe
					ν(Sn—S)	O > NMe > S
1b, **2b**, **3b** (Hal = Br)	BO(X··Sn)	S > O	$\delta(^{119}Sn)^b$	O > S	$d(Sn-Hal)^b$	O > S
	BO(Sn—Hal)	S > O	$^3J(^{13}C-^{119}Sn)^a$	NMe ≫ O > S	$d(Sn-S)^b$	O > S
	Δf(Sn—Hal)	NMe ≫ S = O			ν(Sn—Hal)	O > S ≫ NMe
					ν(Sn—S)	O > NMe > S
1c, **2c**, **3c** (Hal = I)	BO(X··Sn)	S > O	$\delta(^{119}Sn)^b$	O > S	$d(Sn-Hal)^b$	O > S
	BO(Sn—Hal)	S ≫ O	$^3J(^{13}C-^{119}Sn)^{a,b}$	O > S	$d(Sn-S)^b$	O > S
	$\Delta f(Sn-Hal)^c$	NMe ≫ O			$\nu(Sn-Hal)^c$	O ≫ NMe
					$\nu(Sn-S)^c$	O > NMe

[a] Should be described as $^2J(Sn\cdot\cdot N-^{\delta}CH_2)$. [b] No value for donor NMe available. [c] No value for donor S available.

NMR Data. Regarding the ^{119}Sn-NMR chemical shifts of the concerned compounds, it should first be stated that Scheme 1 qualitatively presents an explanation for the well-known effect[27] of a distinct high-field shift by increasing the coordination of tin: the "path" accounts for an enhanced charge density on the tin nucleus and a low-lying LUMO. The high-field shift of coordinatively expanded tin is usually only given as a fact without attempts at a meaningful explanation.[27,28] For a little more detailed discussion, see ref 29.

The last column of Table 4 shows that $\delta(^{119}Sn)$ uniformly follows a high-field direction for the three series **4**, **5**, and **7** from the literature (apart from a small high-field shift for **4d**); obviously the decreasing electronegativity dominates. The behavior of the series of this study deserves more attention. A distinct high-field signal (Hal = Cl) is followed by a distinct low-field shift (Hal = Br) and a tremendous high-field shift (Hal = I). The first low-field shift demonstrates the counterbalancing of electronegativity and lone pair interaction discussed above. The following strong high-field shift if the so-called "heavy-atom effect".[27] Both iodine atoms, the axial one and the equatorial one, relativistically lower the LUMO[30] of Scheme 1 and decrease the ΔE of the paramagnetic term of the NMR shielding theory.[27] The same relativistic drop of the LUMO[30] accounts for the golden yellow color of the iodine compounds.

Influence of the Donor Atom. Table 6 summarizes the distances and stretching vibrations for the equatorial ligands of series **1**–**3**. Shorter distances in comparison with those of an undisturbed tetrahedron (footnote *a* in Table 3) and increased stretching vibrations (footnote *b* in Table 4 and ref 32) support the lowering of σ_{eq} (sp^2) in Scheme 1. Details will be discussed along with the sequence of the donor strength for NMe, O, S. This sequence is evaluated in Table 7 by means of several data. From data concerning the axial ligands, a sequence of the donor strength in the order NMe > S ≥ O can be concluded. The difference between sulfur and oxygen seems to be small and, not amazingly, the sequence NMe > O > S holds in terms of solution NMR data. The conclusion from the data for the equatorial ligands is reversed and nonuniform: O > S > MMe; O > NMe > S. Possibly an intermolecular connection $Sn-Hal_{eq}\cdot\cdot Sn'$ can account for the weak bond $Sn-Hal_{eq}$ in the three cases of the donor NMe. An intermolecular interaction was suggested above due to the low solubilities and high melting points of these compounds. However, if such an interpretation were correct, the bonds $Sn-S_{eq}$ would not be also weak. One explanation for the inconsistency can be that in Scheme 1 no detailed splitting of the equatorial orbitals has been considered, as this is beyond the potential of a qualitative description.

Conclusion

In a qualitative fashion, Scheme 1 approximately accounts for the structural and spectroscopic data for the three investigated compound series and for those of the five series taken from the literature. For a more detailed understanding, especially of how the "equatorial" ligands influence the "path", more data from suitable compound series are needed.

Experimental Section

General Procedures. Starting compunds $O/S(CH_2CH_2SH)_2$ were purchased (Aldrich M380-9 and M400-7). Elemental analyses were carried out by the Microanalytical Laboratory of the Institut für Organische Chemie, Universität Mainz. Mass spectra were taken on a Finnigan 8230 spectrometer. FT-IR spectra were recorded on a Mattson Galaxy 2030 spectrometer (samples pressed disks with polyethylene); Raman spectra, on a spectrometer Spex 1403 (excitation by He/Ne laser (633 nm) or Kr laser (647 nm); samples microcrystalline in capillaries). ^{13}C- and ^{119}Sn-NMR spectra were recorded on a Bruker WP-80/DS FT-NMR spectrometer at 20.15 (^{13}C) and 29.88 (^{119}Sn) MHz (solvents $CDCl_3$ and CD_2Cl_2; external standard $SnMe_4$).

Preparation of Methylbis(2-mercaptoethyl)amine, $MeN(CH_2CH_2SH)_2$. The synthesis was carried out as given in the literature: (1) chlorination of $MeN(CH_2CH_2OH)_2$ (Aldrich M4, 220-3) with $SOCl_2$ in $CHCl_3$;[8] (2) addition of thiourea in ethanol;[9] (3) cleavage of urea by means of aqueous sodium hydroxide (20%).[9] The refluxing with thiourea in step 2 is described for a period of 3 h.[9] Considerably longer refluxing is needed (14 h); further, passing of dry hydrogen chloride through the reaction mixture did not increase the yield of the product. A clear colorless liquid of a repulsive odor is obtained; bp (12 mbar) 98–101 °C.

Preparation of the Dihalogen Stannocanes. Three variants were employed, heating of the tin halide with the free dithiol in $CHCl_3$ (method A[33]) and with a suspension of disodium dithiolate in toluene (method B) and in ethanol (method C[5]). Table 8 summarizes the results obtained by one or the other of these methods.

Structure Determinations. Single crystals were obtained from benzene (**2b**), CCl_4 (**2c**), $CHCl_3$ (**3b**), and toluene (**3c**). All attempts

---

(27) Harris, R. K.; Kennedy, J. D.; McFarlane, W. In *NMR and the Periodic Table*; Harris, R. K., Mann, B. E., Eds.; Academic Press: London, New York, San Francisco, 1978; p 309. Harris, R. K. In *The Multinuclear Approach to NMR Spectroscopy*; Lambert, J. B., Riddell, F. G., Eds.; D. Reidel: Dordrecht, Boston, Lancaster, 1983; p 343., Kennedy, J. D.; McFarlane, W. In *Multinuclear NMR*; Mason, J., Ed.; Plenum Press: New York, London, 1987; p 305.

(28) Harrison, P. G. In *Chemistry of Tin*; Harrison, P. G., Ed.; Blackie: Glasgow, London, 1989; p 76.

(29) Wrackmeyer, B. *Annu. Rep. NMR Spectrosc.* **1985**, *16*, 73.

(30) Pyykkö, P. *Chem. Rev.* **1988**, *88*, 563.

(31) Jensovsky, L. *Z. Chem.* **164**, *4*, 75.

(32) Single-bond Sn—S stretching vibration for comparison: (a) Harrison, P. G.; Stobart, S. R. *J. Organomet. Chem.* **1973**, *47*, 89 (solid phase value of $Me_2Sn(SMe_3)_2$: IR 347, Raman 340 cm^{-1}). (b) Davidovics, G.; Mille, G.; Delmas, M.; Chouteau, J. *J. Mol. Struct.* **1973**, *16*, 59 (five-membered ring $Me_2Sn(SCH_2)_2$, marked splitting: IR 368 and 330 (solution), Raman 354 and 306 cm^{-1} (solid)).

(33) Engler, R. *Z. Anorg. Allg. Chem.* **1974**, *406*, 74; **1974**, *407*, 35.

Table 8. Preparation Details and Analytical Data for the Dihalogen Stannocanes

compd	method	mmol of $SnHal_4$/ solvent (cm^3)	mmol of ligand/ solvent (cm^3)	time (h)	yield (%)	formula	M_r	*m/e* (%)	color	mp (°C)	anal. found (calcd)				
											% C	% H	% S	% N	% Hal
1a	B	10/toluene (100)	10/toluene (100)	14	37	$C_5H_{11}Cl_2NS_2Sn$	338.89	339^b (3)	colorless	249	17.89	3.05	18.92	4.04	20.72
											(17.72)	(3.27)	(18.92)	(4.13)	(20.92)
2a[a]	A	10/$CHCl_3$ (500)	10/$CHCl_3$ (100)	80	86	$C_4H_8Cl_2OS_2Sn$	325.84		colorless	158			21.28		*f*
											(14.74)	(2.47)	(19.68)		(21.76)
3a[a]	A	10/$CHCl_3$ (200)	10/$CHCl_3$ (30)	64	77	$C_4H_8Cl_2S_3Sn$	341.90		colorless	164			29.16		*f*
											(14.05)	(2.36)	(28.13)		(20.74)
1b	B	10/toluene (100)	10/toluene (100)	14	31	$C_5H_{11}Br_2S_2Sn$	427.78	428^b	pale yellow	271	14.00	2.77	14.98	3.28	36.67
											(14.04)	(2.59)	(14.99)	(3.27)	(37.36)
2b	A	25/$CHCl_3$ (125)	25/$CHCl_3$ (125)	69	77	$C_4H_8Br_2OS_2Sn$	414.74	415^b (24)	pale yellow	128–129	12.01	1.84	15.87		*f*
											(11.58)	(1.94)	(15.46)		(38.53)
3b	A	25/$CHCl_3$ (125)	25/$CHCl_3$ (125)	60	59	$C_4H_8Br_2S_3Sn$	430.80	432^b (41)	pale yellow	165	11.84	1.92	22.42		*f*
											(11.15)	(1.87)	(22.33)		(37.09)
1c	C	10/toluene (100)	10/ethanol (100)	4	29	$C_5H_{11}I_2NS_2Sn$	521.78	396^c (100)	gold yellow	187^d	11.62	2.12	12.01	2.74	49.17
											(11.51)	(2.13)	(12.29)	(2.68)	(48.64)
2c	C	16/benzene (400)	16/ethanol (100)	4	12	$C_4H_8I_2OS_2Sn$	508.74	383^c (100)	golden yellow	117	10.25	1.72	12.83		*f*
		16/ethanol (200)	16/ethanol (100)	4	53				golden yellow	117	(9.44)	(1.59)	(12.60)		(49.89)
3c	C	16/benzene (400)	16/ethanol (100)	4	40	$C_4H_8I_2S_3Sn$	524.80	$399^{c,e}$	golden yellow	60^d	10.54	1.83	18.13		*f*
											(9.15)	(1.54)	(18.33)		(48.36)

[a] Ref. 33. The shown results are obtained in this study. [b] M^+. [c] M^+-1. [d] Decomposition. [e] Highest mass 501 (10) corresponding to M^+-2 (CH) (presumably $I_2(SH)SnSCH_2CH_2SH$). [f] Hal not determined.

Table 9. Crystallographic Data for $Br_2Sn(SCH_2CH_2)_2O$ (**2b**) and $I_2Sn(SCH_2CH_2)_2O$ (**2c**) and Structure Determination Details

	2b	**2c**
Crystal Data (Mo Kα_1 λ = 0.709 26 Å)		
formula, M_r	$C_4H_8Br_2O_1S_2Sn$, 414.76	$C_4H_8I_2O_1S_2Sn$, 508.76
crystal habit, color	large square stone, colorless	rhombic plate, colorless
face indices (dist from a common origin inside the crystal, mm)	100, $\bar{1}00$ (0.68) 110 (0.40) $\bar{1}\bar{1}0$ (0.27) $1\bar{1}0$ (0.32) $\bar{1}10$ (0.48)	100, $\bar{1}\bar{1}0$ (0.08) 010, $0\bar{1}0$ (0.06) $00\bar{1}$, 001 (0.08) $\bar{1}01$, $10\bar{1}$ (0.04)
crystal system, space group	orthorhombic, *Cmc*2_1 (No. 36)	monoclinic, *P*2_1 (No. 4)
unit cell dimens		
a, Å	8.763(2)	7.063(1)
b, Å	12.067(2)	12.825(1)
c, Å	10.177(1)	7.269(1)
β, deg		115.79(1)
least-squares fit	29 reflns, θ = 26–30°	50 reflns, θ = 22–27°
packing: *V*, *Z*, *F*(000)	1076(1) Å^3, 4, 768	593(1) Å^3, 2, 456
D_{calcd}, D_{exptl}, g cm^{-3}	2.560, 2.529	2.850, 2.855
Intensity Data Collection (Mo Kα, λ = 0.710 69 Å, Graphite Monochromator)		
temp, °C; θ range, deg	22; 1–35.0	21; 1.5–30.0
$(\sin\theta)_{max}/\lambda$, Å^{-1}	0.8071	0.7035
range of *hkl*	+14, +19, +16	+9, +16, ±9
ref reflns	3, every 3000 s	3, every 4000 s
loss of intensity (time)	3% (2 days)	3% (3 days)
cor	direct fit	linear fit
no. of reflns measd, indep (int B)	1286, 1286	1276, 1137 (0.03)
no. of reflns used, limit	1005, $I > 2\sigma(I)$	1085, $I > 2\sigma(I)$
µ, cm^{-1}; abs cor	98.01; by face indices	74.38; by face indices
range of transm	0.0520–0.0038	0.4622–0.3701
Refinement		
choice of thermal params	Sn, Br, S, C anisotropic; H isotropic fixed	Sn, I, S, C anisotropic; H isotropic fixed
no. of variables; ratio reflns/var	54; 19	93; 11
last shifts	$<0.001\sigma$	$<0.001\sigma$
final, *R*, R_w	0.0494, 0.0648	0.0285, 0.0332
enantiomorphism (signif >99.5%)	R_{w2}/R_{w1} = 1.100	R_{w2}/R_{w1} = 1.072
weighting scheme w^{-1}	$\sigma^2(F) + 0.000979F^2$	$\sigma^2(F) + 0.000446F^2$
final diff Fourier max, e/Å^3	1.6, near Sn	1.0, near Sn

to acquire single crystals from the compound series **1** (X = NMe) failed. Crystal data as well as details of intensity data collections and refinements are given in Tables 9 and 10. The densities were obtained from neutral buoyancy in $CHCl_3/CHBr_3$ for the bromine compounds and in $CHBr_3/CH_2I_2$ for the iodine compounds. The crystals were fixed by gravity and sealed in small glass capillaries. The quality and the symmetry of the crystals were examined by Weissenberg exposures. Integrated intensities were measured by means of $\omega/2\Theta$ scans on a CAD4 diffractometer (Enraf-Nonius). The structures were solved by Patterson syntheses (Sn, Hal) and completed by Fourier syntheses (C, O, S). Hydrogen atoms were calculated and considered as riding on carbon atoms. The refinements resulted in good convergences and in even distributions of the variances. For compound **2b**, Sn, Br, and O were placed on a mirror plane of the space group *Cmc*2_1. Compounds **2b** and **2c** both crystallized in noncentrosymmetric space groups (*Cmc*2_1 and *P*2_1). To prove the significance of the chosen enantiomers, all coordinates were inverted for both compounds; the ratios of the weighted *R*'s are 1.100 for **2b** and 1.072 for **2c**, corresponding to a significance level of 99.5%. Besides several locally written routines, local versions of SHELX-76 and SHELX-86 were used for the calculations and ORTEP was used for drawing the structures. Calculations were done on an IBM RISC/6000.

Table 10. Crystallographic Data for $Br_2Sn(SCH_2CH_2)_2S$ (**3b**) and $I_2Sn(SCH_2CH_2)_2S$ (**3c**) and Structure Determination Details

	3b[a]	**3c**
	Crystal Data (Mo $K\alpha_1$, $\lambda = 0.709\ 26$ Å)	
formula, M_r	$C_4H_8Br_2S_3Sn$, 430.82	$C_4H_8I_2S_3Sn$, 524.82
crystal habit, color	flat square stone, colorless	irregular square stone, yellow
face indices (dist from a common origin inside the crystal, mm	100, $\bar{1}00$ (0.24) 010, $0\bar{1}0$ (0.11) 001, $00\bar{1}$ (0.09)	100, $\bar{1}00$, (0.12, 0.16) 010, $0\bar{1}0$ (0.1, 0.07) 101, $\bar{1}0\bar{1}$ (0.3, 0.23) $10\bar{1}$ (0.40)
crystal system, space group	orthorhombic, *Pbca* (No. 61)	monoclinic, $P2_1/n$ (no. 14)
unit cell dimens		
a, Å	11.271(1)	12.038(1)
b, Å	13.641(1)	13.959(1)
c, Å	14.051(1)	7.175(1)
β, deg		90.88(3)
least-squares fit	45 reflns, $\theta =$ 20−27°	43 reflns, $\theta =$ 24−27°
packing: *V*, *Z*, *F*(000)	2160(1) Å^3, 8, 1527	1191(1) Å^3, 4, 944
D_{calcd}, D_{exptl}, g cm^{-3}	2.649, 2.523	2.927, 2.916
	Intensity Data Collection (Mo $K\alpha$, $\lambda = 0.710\ 69$ Å, Graphite Monochromator)	
temp, °C; θ range, deg	20; 1−27.5	20; 1−27.5
$(\sin \theta)_{max}\ \lambda$, Å^{-1}	0.6497	0.6497
range of *hkl*	+14, +17, +18	+15, +18, ±9
ref reflns	3, every 4000 s	3, every 5000 s
loss of intensity (time)	5% (4 days)	3% (4.5 days)
cor	linear fit	linear fit
no. of reflns measd, indep (int *R*)	2478, 2478 (0.0)	2858, 2735 (0.0255)
no. of reflns used, limit	1797, $I > 2\sigma(I)$	2409, $I > 2\sigma(I)$
μ, cm^{-1}; abs cor	49.70; none	75.61; none
	Refinement	
choice of thermal params	Sn, Br, S, C anisotropic; H isotropic fixed	Sn, I, S, C anisotropic; H isotropic fixed
no. of variables; ratio reflns/var	93; 19	92; 26
last shifts	$<0.001\sigma$	$<0.001\sigma$
final *R*, R_w	0.0467, 0.0808	0.0582, 0.0834
weighting scheme w^{-1}	$\sigma^2(F) + 0.031456F^2$	$\sigma^2(F) + 0.000912F^2$
final diff Fourier max, e/Å^3	1.3, near Sn	2.6, near Sn

[a] Isostructural with **3a**.

Acknowledgment. We are grateful for financial assistance from the Deutsche Forschungsgemeinschaft, Bonn/Bad Godesberg, Germany, and from the Fonds der Chemischen Industrie, Frankfurt/Main, Germany. We thank Bernard Jousseaume, Université Bordeaux I, Talence, France, for compounds **4**, Klaus Jurkschat, Universität Halle-Wittenberg, for compounds **5**, Uwe Bunz, MPI für Polymerforschung, Mainz, Germany, for ^{13}C-NMR spectra, and Terence N. Mitchell, Universität Dortmund, for ^{119}Sn-NMR spectra.

Supplementary Material Available: Tables of atomic coordinates, anisotropic displacement parameters, hydrogen atom positions, bond lengths, bond angles, torsion angles, and vibrational data (12 pages). Ordering information is given on any current masthead page.